Journal of Geophysical Research-Atmospheres

Supporting Information for

Spatiotemporal controls on observed daytime ozone deposition velocity over Northeastern U.S. forests during summer

O. E. Clifton[1,2], A. M. Fiore[1], J. W. Munger[3], R. Wehr[4]

[1]Department of Earth and Environmental Sciences, Columbia University, and Lamont-Doherty Earth Observatory of Columbia University, Palisades, NY, USA.

[2]Advanced Study Program, National Center for Atmospheric Research, Boulder, CO, USA.

[3]Division of Engineering and Applied Science and Department of Earth and Planetary Sciences, Harvard University, Cambridge, MA, USA.

[4]Department of Ecology and Evolutionary Biology, University of Arizona, Tucson, AZ, USA.

Corresponding Author: O. E. Clifton, Advanced Study Program, National Center for Atmospheric Research, Boulder, CO, USA (oclifton@ucar.edu).

Contents of this file

Text S1 to S8

Figure S1

Table S1 to S2

Introduction

Text S1 details the ozone deposition velocity calculation and filtering techniques used.

Text S2 details leaf area index measurements at all three forests.

Text S3 describes soil moisture measurements at Harvard Forest.

Text S4 describes the stomatal conductance models used.

Text S5 provides information on the bootstrapping technique.

Text S6 provides details of the multiple linear regression analyses used for day-to-day variability.

Text S7 details the ozone dry deposition model from Massman (2004).

Text S8 describes the regression for the temperature dependence of the observed ozone fluxes.

Figure S1 shows the difference in monthly mean ozone deposition velocity at Harvard Forest for 1998 and 1999 due to filtering technique.

Table S1 shows the mean and standard deviation used for removing high and low ozone deposition velocities at the short-term monitoring sites and Harvard Forest (only used for Harvard Forest when comparing to the short-term sites).

Table S2 provides the details of the linear regression models described in Text S8.

Text S1

Ozone deposition velocity calculation and filtering techniques used.

For Kane and Sand Flats, 30-minute mean ozone fluxes are given in ppb m s^{-1} and ozone concentrations from the fast sensor are given in ppb. We calculate ozone deposition velocity (v_d) by dividing the flux by the concentration of the fast analyzer. We assume that the fluxes at Kane and Sand Flats are calculated using air density that varies with virtual temperature (T_v) and pressure. At Sand Flats, there are 17 erroneous temperature measurements (e.g., T_v greater than 100ºC and T_v less than -10ºC during the growing season) that have not been discarded; we discard the corresponding values of v_d.

For Harvard Forest, fluxes are given hourly and in μmol m^{-2} s^{-1}. Concentrations from the fast ozone analyzer are given in ppb. We convert the fluxes to ppb m s^{-1} using constant air density at 25ºC and 1013 hPa because there are extended periods with missing air temperature measurements (e.g., all of 1990 and most of 1991). We find that calculating v_d with constant air density leads to a mean offset of 0.01 cm s^{-1} at Harvard Forest as compared to varying air density with air temperature at constant pressure (987 hPa), which was the approach used to calculate the fluxes (Clifton et al., 2017). Thus, using constant air density at Harvard Forest but varying air density at Kane and Sand Flats should only have a minor impact on our comparison.

At Harvard Forest, the ozone fluxes are computed half-hourly and then averaged to hourly and reported as hourly. We average Kane and Sand Flats ozone fluxes and concentrations from half-hourly to hourly before calculating v_d to ensure consistency in our comparison of the data among sites.

For Harvard Forest, we follow the same method as Clifton et al. (2017) for removing outliers. This method is: we remove outliers by requiring hourly v_d to fall within the mean ± three standard deviations of the entire hourly time series (i.e., we retain 99.7% of the data; $\mu = 0.28$ cm s^{-1} and $\sigma = 0.50$ cm s^{-1}). Before doing this, we remove any periods with ozone fluxes that correspond to missing latent and sensible heat fluxes as in Clifton et al. (2017) because often these periods correspond to near-zero ozone fluxes. In addition, in this paper, we remove any other extended time periods with near-zero v_d (November 27, 1990 at 22:00 EST to November 29, 1990 at 0:00; September 4, 1999 at 14:00 to September 5, 1999 at 10:00; November 20, 1992 at 12:00 to November 23, 1992 14:00; October 28, 1992 16:00 to October 31, 1992 at 11:00) before filtering, which does not change the μ or σ. We refer to this method as the Clifton et al. (2017) filtering method.

Except where stated otherwise, we use this filtering method for Harvard Forest. This filtering method applies equally to all years and is thus appropriate to compare v_d across the years at Harvard Forest. Howev-

er, this filtering approach is not appropriate for comparisons between v_d at Harvard Forest and the short-term monitoring sites, which only have data for the growing season when v_d is relatively high (i.e., μ would be much higher at the short-terms sites). Therefore, when we compare Harvard Forest and Kane 1997 data and Harvard Forest and Sand Flats 1998 data directly in Figure 1, we filter hourly v_d for 1997 and 1998 by the $\mu \pm 3\sigma$ of the 1997 and 1998 growing seasons, respectively (see Table S1 for the μ or σ at each forest and time period). We define the growing season for 1997 and 1998 as the observing periods at Kane (April 29 to October 23, 1997) and Sand Flats (May 12 to October 20, 1998), respectively. Before filtering, we remove hourly $|v_d|$ greater than 10 cm s^{-1} at each forest as there is are ten such values at Kane and one at Sand Flats. The magnitude of v_d changes with the filtering approach used, especially for 1997 and 1998 at Harvard Forest (Figure S1), as these are high v_d years and they have more data filtered out by the Clifton et al. (2017) method. When we compare Harvard Forest, Sand Flats and Kane directly in Figure 1, we use the filtering approach described in this paragraph. We retain this filtering method for Kane and Sand Flats for the rest of the paper, but elsewhere for Harvard Forest we use the Clifton et al. (2017) method.

Text S2

Leaf Area Index at Harvard Forest.

Leaf Area Index (LAI) measurements are available from 1998, 1999 and 2005-2014 (Munger & Wofsy, 1999a; Barford et al., 2001). LAI is measured using a LICOR 2000 plant canopy analyzer. We use LAI averaged across 1998, 1999 and 2005-2014. In our estimate, we include plots A through H except G3, H3, and H4, which only have data for a couple of years. LAI is measured at several plots in the dominant wind sectors of the EMS tower: the northwest (NW) and southwest (SW). We average across the plots in each wind sector, interpolate to daily resolution and average across years. LAI differs between these wind sectors consistently (by 0.9 m^2 m^{-2} on a multiyear mean basis). In order to capture the LAI of the flux tower footprint in models requiring input at hourly time resolution, we repeat the daily estimate for each hour of the day, and use NW LAI when wind comes from the NW and SW LAI when wind comes from the SW. When wind comes from the east, we use LAI from the SW wind sector.

For models requiring LAI as input, we choose to include 2005-2014 in addition to 1998-1999 in the multiyear average to dampen interannual variability in LAI (±10%), especially because there is low LAI during 1998 due to stunted canopy growth (Urbanski et al., 2007). We note that canopy tree biomass has increased from 1990 to 2010 by one third (Eisen & Plotkin, 2015). Another model that we use and employs LAI is the Wehr and Saleska (2015) empirical stomatal conductance model, which is described in Text S4. The multiyear mean LAI used in this estimate differs slightly from our other calculations, but also accounts for varying LAI with wind direction (Wehr & Saleska, 2015; see their Appendix B4).

Leaf Area Index at Kane and Sand Flats.

LAI is measured using a LICOR 2000 plant canopy analyzer (Meyers et al., 1998; Finkelstein, 2001). Finkelstein et al. (2000) multiply the LAI by a correction factor (Chason et al., 1991) to account for clumping of leaves, but we do not use a clumping factor at Harvard Forest, Kane or Sand Flats. LAI is homogeneous around the flux tower at Kane, but heterogeneous around the flux tower at Sand Flats (Finkelstein et al., 2000). The predominant wind sectors at Sand Flats are the southwest and the southeast; LAI is higher in the southwest (for more information see Finkelstein et al. (2000) Section 3.1). To give the reader a sense of how much LAI varies by wind sector at Sand Flats, maximum LAI is 3.74 m^2 m^{-2} and minimum is 2.44 m^2 m^{-2} during June-September 1998. We use hourly LAI at Sand Flats that varies with observed wind direction to represent the instrument footprint of the flux tower.

Text S3

Soil Moisture at Harvard Forest.

Volumetric soil moisture measurements (top 15 cm of soil) are available for 1995 to 2000 (Davidson & Savage, 1999; Savage & Davidson, 2000). We use the measurement plots: NWF, NWM, NWN, SWF, SWM, and SWN. The first two letters correspond to the wind sector (northwest or southwest), and the last letter corresponds to distances far (F), mid (M), and near (N) the tower (see Table 1 of Davidson et al. (1998)). We linearly interpolate soil moisture for each plot from approximately weekly to daily.

Text S4

Stomatal conductance models.

For Harvard Forest, we use three observation-driven estimates of stomatal conductance (g_s). The first two are modified slightly from Clifton et al. (2017).

Inversion of Penman-Monteith

The first g_s estimate employs water vapor EC fluxes; it is the Shuttleworth et al. (1984) inversion of the Penman-Monteith equation (hereafter, P-M):

$$g_s = ((\frac{\Delta' \lambda}{c_p}\beta - 1)R_a + \frac{\rho_a \lambda (q_w(T_a) - q)}{\lambda E})^{-1} \text{ (S1)}$$

Δ' is the slope of the saturated humidity curve for air temperature T_a (Allen et al., 1998); λ is latent heat of vaporization of water (2442 kJ kg^{-1}); E is water vapor eddy covariance flux; we correct the specific heat capacity at constant pressure (c_p; 1010 J K^{-1} kg^{-1}) for moist air; ρ_a is air density at 25ºC and 1013 hPa; β is the Bowen ratio ($H/\lambda E$) where H is sensible heat flux; $q_w(T_a)$ is saturation specific humidity at T_a; and q is specific humidity. R_a is the aerodynamic resistance (see Text S7). We scale g_s for water vapor from Equation (S1) by the ratio of ozone diffusivity to water vapor diffusivity (0.66; Massman, 1998).

The following paragraph describes modifications to the P-M inversion from Clifton et al. (2017). In P-M, we account for sub-canopy evapotranspiration by removing 10% of the hourly observed water vapor flux value (Moore et al., 1996), before including the term in P-M. This value was calculated by Moore et al. (1996) using short-term above and below canopy flux measurements, and using this value as a summertime average is corroborated by Wehr et al. (2017) who infer the evaporation fraction of evapotranspiration at Harvard Forest using flux and isotope measurements. We acknowledge that assuming evaporation is always 10% of evapotranspiration is likely an oversimplification, but we use two other methods of inferring g_s at Harvard Forest to support our findings with P-M. In Clifton et al. (2017), we applied this change to evapotranspiration in both of its instances in P-M, but here we do not adjust evapotranspiration in the Bowen ratio because this part of the P-M equation represents energy balance. Another change is that we use air density that changes with ambient temperature and pressure instead of using constant air density. The third modification is that we use wind-direction dependent LAI (see Text S2) in R_a. Fourth, we do not include hourly P-M g_s with atmospheric vapor pressure deficit (VPD) less than 0.5 kPa as the estimate generally becomes unreliable at high humidity. Previous observational studies also exclude water-flux-based g_s estimates with high ambient humidity, employing various thresholds (Hogg et al., 2007; Lamaud et al., 2009; Rannik et al., 2012; Launiainen et al., 2013; Novick et al., 2016). We select 0.5 kPa because this threshold more or less optimizes the relationship between v_d and g_s on daily timescales investigated in Section 3.2. These changes do not alter the conclusions of Clifton et al. (2017).

For P-M, we do not exclude days with rain from our analysis. We acknowledge that P-M has serious shortcomings after rain due to the enhanced contribution of evaporation to evapotranspiration. However, because we examine lower-frequency averages, we wish to retain as much data as possible. To build confidence in our results using P-M, we compare them to the findings using the two other g_s estimates described below.

Optimal photosynthesis, minimal transpiration model

The second g_s estimate is obtained from an optimal photosynthesis, minimal transpiration model (Lin, Y. S., et al., 2015; Medlyn et al., 2011; hereafter, "L15").

$$g_s = \frac{1}{n_a}(1 + \frac{g_1}{\sqrt{VPD}})\frac{A_{net}}{C_{CO_2}} \quad \text{(S2)}$$

n_a is the number density of air at 25ºC and 1013 hPa; g_1 is a constant, inversely proportional to the square root of the cost of carbon per unit water used by the plant; VPD is atmospheric vapor pressure deficit; A_{net} is net photosynthesis rate; and C_{CO_2} is the carbon dioxide mixing ratio. For this model, we employ gross primary productivity (GPP) as the best estimate of net photosynthesis. GPP at Harvard Forest is inferred from observed carbon dioxide fluxes; the calculation assumes daytime ecosystem respiration has the same relationship to soil temperature as nighttime (Wofsy et al., 1993; Urbanski et al., 2007). We scale g_s for carbon dioxide from Equation (S2) by the ratio of ozone diffusivity to carbon dioxide diffusivity (1.06). For L15 we do not include hourly values with VPD less than 0.02 kPa because the majority of summer daytime hourly L15 g_s outliers occur when VPD is below 0.02 kPa (Clifton et al., 2017). L15 calculate g_1 for red oak at Harvard Forest as 5.14 by fitting Equation (S2) to short-term leaf-level measurements. For L15, we use $g_1 = 2.61$ for red oak at Harvard Forest (Franks et al., 2018) as this value corrects for the factor of 2-3 overestimate in L15 relative to P-M g_s found by Clifton et al. (2017).

Empirical model

The third g_s estimate is the Wehr and Saleska (2015) empirical model (hereafter, "W15") for g_s at Harvard Forest:

$$g_s = \frac{1}{n_a} LAI(b_0 e^{b_1 LVD} e^{b_2 \chi}) PAR \quad \text{(S3)}$$

This model is a function of LAI, leaf-to-air vapor pressure deficit (LVD), clear sky index (χ), and photosynthetically active radiation (PAR) (Wehr & Saleska, 2015). To allow for long-term trends (e.g., due to LAI), the three free parameters in this model (b_0, b_1, b_2) are tuned such that W15 g_s fits the five-year running average centered on the current year (for 1992 and 1993 only 3 and 4 years are used, respectively) estimated from the measured latent heat flux during periods with minimal evaporation (i.e., excluding

periods after rain and mornings with likely dew, as described in Appendix B4 of Wehr and Saleska (2015)). The estimation of g_s from heat fluxes in this approach is similar to P-M but is closer to the derivation from Fick's Law (see Appendix C of Wehr and Saleska (2015)). We scale g_s for water vapor from Equation (S3) by the ratio of ozone diffusivity to water vapor diffusivity (0.66; Massman, 1998).

Kane and Sand Flats

For Kane and Sand Flats, we only use the P-M g_s estimate because g_1 and GPP for L15 have not been inferred for these sites (doing so is beyond the scope of this manuscript) and W15 was designed specifically for Harvard Forest. Our P-M method for Kane and Sand Flats is the same as for Harvard Forest except where mentioned below. Note that we use the same assumption for the evaporation fraction of evapotranspiration at Kane and Sand Flats as Harvard Forest (10%), but there has been no prior work at these sites to constrain this fraction observationally.

For Kane and Sand Flats, we remove hourly g_s with VPD less than 0.3 kPa. This threshold is less stringent than for Harvard Forest in order to maximize the data available (we only have data for one growing season at these sites). Generally, we remove values with low VPD to optimize the regression of v_d against P-M g_s. We show in Text S6 and Table 1 that our regression results are similar for both thresholds. For Kane and Sand Flats, we remove P-M g_s with hourly rain above zero.

Text S5

Bootstrapping Technique

Whenever we composite a time series of a certain variable, we use a bootstrapping technique to estimate the mean and 95% confidence intervals in order to utilize all of the available data. For each hour, year and/or environmental condition, we create 1000 distributions (i) of n samples of the variable by resampling with replacement where n is the number of days with non-missing data for each hour and year and/or environmental condition. We set the minimum threshold for n to be 25% of the maximum number of days for each year and/or environmental condition. We average across each of these 1000 distributions to obtain 1000 means for each hour, year, and/or environmental condition. Then we create 1000 daytime means for each year and/or environmental condition by averaging the hours from 9am to 4pm at the same index i = 1,…,1000. To create the daytime average, we average across these 1000 values. The 5^{th} to 95^{th} confidence intervals are the 26^{th} to 975^{th} daytime mean values.

Text S6

Multiple linear regression analyses used for day-to-day variability.

Daily anomalies are used in the multiple linear regressions for each site described below.

Harvard Forest.

The following details describe the multiple linear regression model for Harvard Forest. We regress v_d anomalies on relative humidity (RH) and P-M stomatal conductance (g_s) anomalies. The variance inflation factors (VIF) are 1, suggesting that collinearity among predictors (RH and P-M g_s) has little influence on the model. We iterate thrice removing six points that are outliers, or have disproportionate impact on the model (i.e., relatively high Cook's distance or leverage points). In each iteration, we regress then remove the outlier(s) and point(s) with disproportionate impact, and regress again.

Kane Experimental Forest.

The following details describe the multiple linear regression model at Kane for 1997. We regress v_d anomalies on RH and P-M g_s anomalies. VIFs are 1, suggesting that collinearity among predictors (RH and P-M g_s) has little influence on the model. We iterate twice to remove six points that have a disproportionate impact on the model. Table 1 gives the coefficients for each predictor and the y-intercept, the number of observations, the root mean square error, and the adjusted R^2. Having a higher VPD threshold (VPD>0.5 kPa instead of VPD>0.3 kPa) for hourly P-M g_s does not generally change our findings (see Table 1 for VPD>0.3kPa; for VPD>0.5kPa, y-intercept=0.082±0.023 (significant), coefficient for P-M anomaly is 0.452±0.130 (significant), coefficient for RH anomaly is 0.009±0.002 (significant), n is 38, adjusted R^2 is 0.57, root mean squared error is 0.11; here we iterate twice to remove four points that have a disproportionate impact on the model). However, the model results for Kane are more similar to Harvard Forest when VPD>0.3 kPa is employed, which lends confidence to this estimate.

Sand Flats State Forest.

The following details describe the multiple linear regression model at Sand Flats for 1998. We regress v_d anomalies on RH and P-M g_s anomalies, but find that P-M g_s is not a significant predictor for v_d at Sand Flats. We remove five outliers with a disproportionate impact on the model with one iteration. Table 1 gives the coefficients for each predictor and the y-intercept, the number of observations, the root mean square error, and the adjusted R^2. Having a higher VPD threshold (VPD>0.5 kPa instead of VPD>0.3 kPa) for hourly P-M g_s does not change our findings because it does not lead to P-M becoming a significant predictor.

Text S7

Ozone dry deposition estimated with Massman (2004) model.

For the Massman (2004) model, we combine equations (S4)-(S12) to estimate v_d using hourly meteorological and biophysical observations (or quantities inferred from observations).

$$v_d = (R_a + \frac{1}{\frac{1}{R_{b,leaf} + R_{c,leaf}} + \frac{1}{R_{ac} + R_{b,soil} + R_{soil}}})^{-1} \text{ (S4)}$$

$$R_{c,leaf} = \frac{1}{R_s^{-1} + R_{cut}^{-1}} \text{ (S5)}$$

$$R_{cut} = g_{cut}^{-1} = \frac{R_{0,cut}}{LAI} \text{ (S6)}$$

$$R_{ac} = \frac{R_{0,ac} LAI}{u_*} \text{ (S7)}$$

$R_{b,soil}$ is 40 s m^{-1}, R_{soil} is 100 s m^{-1} for dry soil and 500 s m^{-1} for wet soil (distinction between wet and dry soil described in Section 3.3.1), $R_{0,cut}$ is 5000 s m^{-1}, and $R_{0,ac}$ = 25 s m^{-1}, all as prescribed by Massman (2004). The constants are not specific to land cover type. R_a is the aerodynamic resistance and $R_{b,leaf}$ is the resistance to molecular diffusion in the small boundary layer around leaves.

Aerodynamic resistance.

Aerodynamic Resistance (R_a), the resistance posed by above-canopy turbulence, is from Fick's Law:

$$R_a = \frac{1}{k u_*}[ln(\frac{z_r - d}{z_{0,m}}) - \Psi_H(\frac{z_r - d}{L})] \text{ (S8)}$$

k is the von Kármán constant (0.40); u_* is friction velocity; z_r is reference height (29 m); d is zero-plane displacement height; $z_{0,m}$ is roughness length for momentum; and Ψ_H is the stability correction function. The Monin-Obukhov length (L) is:

$$L = \frac{-(u_*)^3}{k g \frac{H}{T_v c_p \rho_a}} \text{ (S9)}$$

g is gravitational acceleration; T_v is virtual temperature; H is sensible heat flux; c_p is specific heat capacity at constant pressure (1010 J K^{-1} kg^{-1}) that we correct for moist air; and ρ_a is air density at 25ºC and 1013 hPa. We use mean canopy height and LAI (see Text S2) to calculate $z_{0,m}$ and d (Wu et al., 2015; Meyers et al., 1998). Ψ_H (Paulson, 1970; Foken, 2008) is an integral form of the dimensionless heat profiles (ϕ_H) (Businger et al., 1971; Högström, 1988). We use ϕ_H summarized as the current understanding of Monin-Obukhov similarity theory by Foken (2006):

$$\Psi_H = 2ln\frac{1 + (0.95(1 - 11.6\frac{z_r - d}{L})^{0.5})}{2}, \frac{z_r - d}{L} \in (-2,0) \text{ (S10)}$$

$$\Psi_H = -7.8\frac{z_r - d}{L}, \frac{z_r - d}{L} \in (0,1) \text{ (S11)}$$

Leaf sublaminar layer resistance.

We calculate the sublaminar layer resistance for leaves ($R_{b,leaf}$) according to Wesely and Hicks (1977):

$$R_{b,leaf} = \frac{2}{k\,u_*}\left(\frac{\kappa}{D_{O_3}}\right)^{2/3} \text{ (S12)}$$

k is the von Kármán constant (0.40); u_* is friction velocity; κ is thermal diffusivity of air (0.2 $cm^2\ s^{-1}$); and D_{O3} is diffusivity of ozone (0.14 $cm^2\ s^{-1}$; Massman, 1998).

Text S8

Linear regression for the temperature dependence of the observed ozone fluxes.

The following details describe the linear regression model for Harvard Forest for hourly ozone fluxes when wind comes from the northwest during June-September 9am-4pm against an exponential function of air temperature ($e^{0.17*(T-30)}$) (Duhl et al., 2008) during 1998, 1999, and all years except 1998 and 1999 with both ozone flux and air temperature measurements. For the first model (1998), we iterate five times removing 16 outliers or points that have disproportionate impact on the model (i.e., relatively high Cook's distance or leverage points). For the second model (1999), we iterate four times removing 27 outliers or points that have disproportionate impact on the model. For the third model (all years except 1998 and 1999), we iterate twice removing 24 points that are outliers, or have disproportionate impact on the model. Table S2 gives the coefficients for the exponential function of air temperature and the y-intercept, the number of observations, the root mean square error, and the adjusted R^2. In each iteration, we regress then remove the outlier(s) and point(s) with disproportionate impact, and regress again.

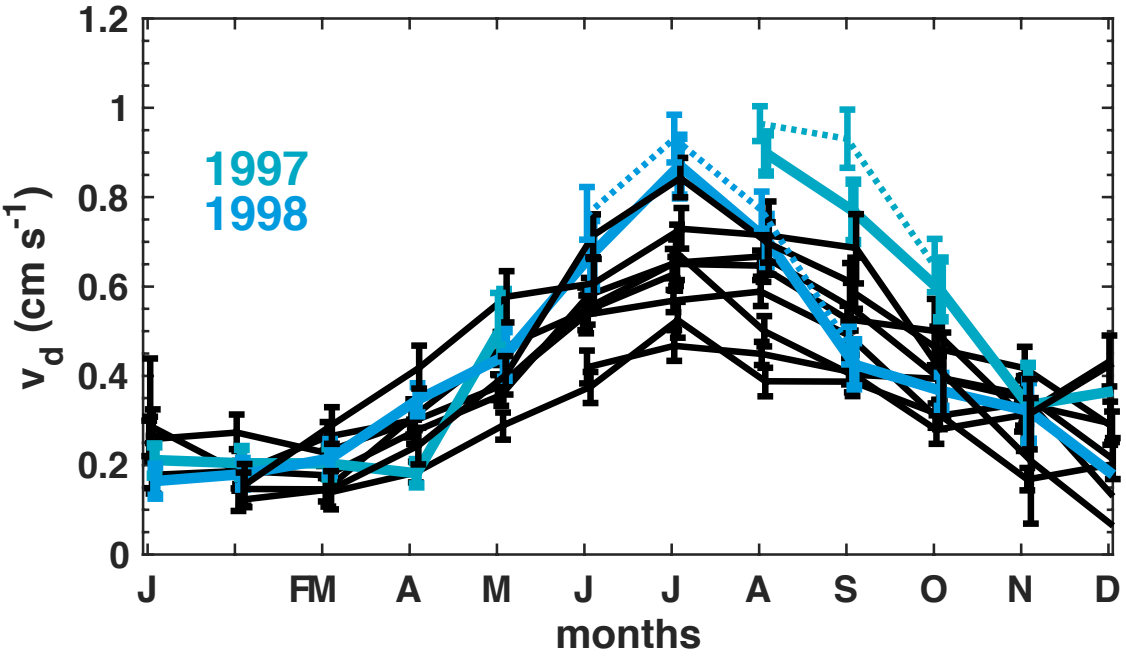

Figure S1. Ozone deposition velocity (v_d) at Harvard Forest. The black lines show monthly daytime (9am-4pm) mean v_d calculated with a bootstrapping method for 1990 to 2000 after we filter hourly values by the mean ± three standard deviations of the entire dataset (Clifton et al., 2017). Solid colored lines show v_d at Harvard Forest for 1997 and 1998, the years when there are observations at nearby forests. Dashed colored lines indicate the monthly daytime mean v_d at Harvard Forest for 1997 and 1998 after we first remove any hourly values with absolute value greater than 10 cm s^{-1} and then filter by the mean ± three standard deviations of all the data in the year's growing season (Table S1), which is defined by the measurement periods of Kane Experimental Forest for 1997 and Sand Flats State Forest for 1998. If the percentage of days with missing data for any hour between 9am and 4pm for any month and year is greater than 75% then that monthly average is not included.

	April 29-October 23 1997	May 12-October 1998
Harvard Forest	$\mu = 0.49$, $\sigma = 0.74$	$\mu = 0.44$, $\sigma = 0.65$
Short-term monitoring site	$\mu = 0.35$, $\sigma = 0.60$ (Kane)	$\mu = 0.39$, $\sigma = 0.50$ (Sand Flats)

Table S1. The mean and standard deviation used to filter the ozone deposition velocities from Harvard Forest, Kane Experimental Forest and Sand Flats State Forest (the latter two are the short-term monitoring sites) during the growing season 1997 and 1998, defined by the measurement periods at Kane and Sand Flats, respectively. We only use these values to filter Harvard Forest ozone deposition velocities when we directly compare Harvard Forest with Kane and Sand Flats (i.e., in Figure 1).

	y-intercept	$e^{0.17*(T-30)}$	n	adjusted R^2	RMSE
All years except 1998 and 1999	*30.8±1.07*	*32.7±3.95*	1264	0.0509	21
1998	*24.9±4.12*	*66.1±17.7*	152	0.0789	18.8
1999	*36.5±3.37*	*62.5±9.15*	245	0.157	26.3

Table S2. Coefficients (estimates±standard errors) for the linear regression of hourly 9am-4pm ozone fluxes (in μmol O_3 m^{-2} s^{-1}) when wind comes from the northwest on an exponential temperature dependence during June through September at Harvard Forest. T is air temperature. n is the number of observations used in the model, RMSE is the root mean squared error. Italics denote $p<0.05$ for predictors. All models are statistically significant ($p<0.05$).